

Detecting quantum chaos via pseudo-entropy and negativity

Song He,^{a,b} Pak Hang Chris Lau,^{c,d} and Long Zhao^a

^a*Center for Theoretical Physics and College of Physics, Jilin University, Changchun 130012, People's Republic of China*

^b*Max Planck Institute for Gravitational Physics (Albert Einstein Institute), Am Mühlenberg 1, 14476 Golm, Germany*

^c*Department of Physics, Osaka University, Toyonaka, Osaka 560-0043, Japan.*

^d*Department of Physics, Kobe University, Kobe-shi, Hyogo 657-8501, Japan*
E-mail: hesong@jlu.edu.cn, u948999a@icho2.osaka-u.ac.jp, zhaolong@jlu.edu.cn

ABSTRACT: Quantum informatic quantities such as entanglement entropy are useful in detecting quantum phase transitions. Recently, a new entanglement measure called pseudo-entropy was proposed which is a generalization of the more well-known entanglement entropy. It has many nice properties and is useful in the study of post-selection measurements. In this paper, one of our goals is to explore the properties of pseudo-entropy and study the effectiveness of it as a quantum chaos diagnostic, i.e. as a tool to distinguish between chaotic and integrable systems. Using various variants of the SYK model, we study the signal of quantum chaos captured in the pseudo-entropy and relate it to the spectral form factor (SFF) and local operator entanglement (LOE). We also explore another quantity called the negativity of entanglement which is a useful entanglement measure for a mixed state. We generalized it to accommodate the transition matrix and called it pseudo-negativity in analogy to pseudo-entropy. We found that it also nicely captures the spectral properties of a chaotic system and hence also plays a role as a tool of quantum chaos diagnostic.

Contents

1	Introduction	1
2	Review of the SYK model and its variants	3
3	Pseudo-entropy as a probe of chaos	6
3.1	Chaotic spectrum via pseudo-entropy	6
3.2	Pseudo-entropy in the subsystem	11
4	The local operator entanglement	15
5	Negativity of entanglement	18
5.1	Pseudo-negativity in binary sparse SYK ₄	20
5.2	Diagrammatic computation	21
6	Summary and prospect	23
A	Diagrammatic approach	25

1 Introduction

The authors in [1, 2] posit that a quantum system suitable for describing a black hole must exhibit quantum chaotic behavior, based on certain general assumptions. This notion finds support in the anti-de Sitter/conformal field theory (AdS/CFT) correspondence [3–5]. According to AdS/CFT, the boundary dual of a black hole geometry in a d -dimensional asymptotically AdS spacetime corresponds to a CFT in a thermofield double (TFD) state in $d - 1$ dimension. By examining the out-of-time-order (OTOC) correlation function in the CFT, one can identify a non-zero Lyapunov exponent which indicates the system is chaotic [6, 7].

According to the discussion in Ref. [8], the OTOC can be used to measure the change of quantum entanglement between a subsystem and its complement. Therefore, one can diagnose quantum chaos by entanglement entropy. Quantum entanglement is another crucial aspect of quantum gravity [9, 10]. Ryu and Takayanagi proposed that the entanglement

entropy of a subregion in the boundary conformal field theory is equivalent to the area of the corresponding minimal surface in the bulk. This connection is known as the holographic entanglement entropy conjecture [11, 12] and is an essential component of the AdS/CFT correspondence framework [13–17]. Besides OTOC, there are also other quantities that serve as probes of quantum chaos, such as the K-complexity [18–27], the energy level spacing distribution, and the Spectral Form Factor (SFF) [28–34], etc. Therefore, it is also interesting to establish connections between these quantities and quantum entanglement.

The pseudo-entropy is a generalization of the entanglement entropy in the sense that entanglement entropy appears as a special case. Entanglement entropy captures the quantum entanglement between a subregion (A) and its complement (\bar{A}) of a pure state. Given a pure state $\rho = |\psi\rangle\langle\psi|$ of a system, the entanglement entropy is defined as the von Neumann entropy of the reduced density matrix $\rho_A = \text{tr}_{\bar{A}}\rho$.

$$S_A = -\text{tr}\rho_A \log \rho_A. \quad (1.1)$$

For the case of pseudo-entropy, a transition matrix between two states $|\psi\rangle$ and $|\varphi\rangle$ is constructed instead of the usual density matrix

$$\mathcal{T}^{\psi|\varphi} = \frac{|\psi\rangle\langle\varphi|}{\langle\varphi|\psi\rangle}, \quad (1.2)$$

where the transition matrix is generally non-hermitian and its trace is normalized to unity. The computation of the pseudo-entropy closely resembles its entanglement entropy counterpart. We first partial trace over a subregion of the transition matrix to obtain the reduced transition matrix

$$\mathcal{T}_A^{\psi|\varphi} = \text{tr}_{\bar{A}}\mathcal{T}^{\psi|\varphi}. \quad (1.3)$$

Then the pseudo-entropy is obtained by substituting this reduced transition matrix into the von Neumann entropy formula

$$S(\mathcal{T}_A^{\psi|\varphi}) = -\text{tr}_A\mathcal{T}_A^{\psi|\varphi} \log \mathcal{T}_A^{\psi|\varphi}. \quad (1.4)$$

Alternatively, it can be computed by the replica trick with the help of a generalized version of the Rényi entropy. The n -th pseudo-Rényi entropy of the transition matrix $\mathcal{T}_A^{\psi|\varphi}$ is defined as

$$S^{(n)}(\mathcal{T}_A^{\psi|\varphi}) = \frac{1}{1-n} \log \text{tr} \left[\left(\mathcal{T}_A^{\psi|\varphi} \right)^n \right], \quad (1.5)$$

where the pseudo-entropy is recovered by taking the $n \rightarrow 1$ limit. There is also substantial research based on the pseudo-entropy [35–37] and its connection to time-like entanglement [38–43], the information paradox through the study of Page curve [44] and 2-dimensional CFT where analytic computation is possible [45–48]. The mathematical structure of transition matrices is more general than that of density matrices. Therefore, pseudo-entropy can be more generally connected to other quantities when compared with the entanglement entropy. The main goal of this paper is to explore further the properties of pseudo-entropy and its application to quantum chaos based on the work [49], where the authors demonstrated that the connection of the pseudo-entropy to the spectral form factor.

In this paper, we will focus on the sparse SYK model, which was first proposed in [50, 51]. It is a modification of the original SYK model which contains an interesting feature of chaos/integrable transition. There have been many works studying this modified model through the use of spectral form factor [52] and OTOC [53]. Besides as a model of quantum chaos, it has also been used as a simple model for modeling a transversable wormhole [54, 55]. One can further simplify the sparse SYK model by restricting the allowed value of the coupling constants to ± 1 and it becomes the binary sparse model [56]. The advantage of this much-simplified model is that it retains the essential features of the original model but is more numerically efficient. We will also take advantage of it and study the properties of pseudo-entropy and negativity using this model.

The structure of this paper is as follows. In Section 2 we give an overview of the SYK model and its variants. In Section 3, we derive the relationship between the SFF and the pseudo-Rényi entropy. In Section 4, we establish the relationship between the pseudo-Rényi entropy and the OTOC. In Section 5, we study the negativity of a transition matrix, namely pseudo-negativity. We end in Section 6 with a summary and an outlook.

2 Review of the SYK model and its variants

The SYK model is a q -body all-to-all interacting theory of N Majorana fermions. Its full Hamiltonian is [57–59]

$$H = i^{q/2} \sum_{1 \leq i_1 < \dots < i_q \leq N} J_{i_1 \dots i_q} \psi_{i_1} \cdots \psi_{i_q}, \quad (2.1)$$

where the Majorana fermions, ψ , satisfy the anticommutation relation $\{\psi_i, \psi_j\} = 2\delta_{ij}$, the coupling tensor $J_{j_1 j_2 \dots j_q}$ is totally antisymmetric, and each independent element is

randomly drawn from a Gaussian distribution with zero mean and variance $\langle J_{j_1 j_2 \dots j_q}^2 \rangle = \frac{(q-1)!}{N^{q-1}} J_0^2 = \frac{2^{q-1}(q-1)!}{qN^{q-1}} \mathcal{J}^2$.

The spectral statistics of the SYK model can be effectively described by Random Matrix Theory (RMT). Specifically, in the case where q modulo 4 is equal to 0, the spectral statistics fall under the Gaussian Orthogonal Ensemble (GOE) for N modulo 8 equal to 0, the Gaussian Symplectic Ensemble (GSE) for N modulo 8 equal to 4, and the Gaussian Unitary Ensemble (GUE) for N modulo 8 equal to 2 or 6 [29]. On the other hand, in the case where q modulo 4 is equal to 2, the spectral statistics belongs to Class C (BdG) for N modulo 8 equal to 4 and Class D (BdG) for N modulo 8 equal to 0 [30, 60, 61].

Recently, a sparse version of the SYK model was proposed [50]. The full Hamiltonian of the sparse SYK $_q$ model with N Majorana fermions [50] is given by

$$H = i^{q/2} \sum_{1 \leq i_1 < \dots < i_q \leq N} x_{i_1 \dots i_q} J_{i_1 \dots i_q} \psi_{i_1} \dots \psi_{i_q}, \quad (2.2)$$

where the parameters $x_{i_1 \dots i_q}$ are chosen to be 1 with probability p and 0 with probability $1 - p$. The number of non-zero terms in the sum (2.2) is approximately given by

$$k_{cpl} = p \binom{N}{q} \approx \frac{pN^q}{q!}. \quad (2.3)$$

The amount of the sparseness of the model is controlled by the parameter

$$k = k_{cpl}/N \approx \frac{pN^{q-1}}{q!}. \quad (2.4)$$

This sparse version of the SYK model has been proven that it exhibits chaotic behavior when k exceeds a certain $\mathcal{O}(1)$ constant [50, 51]. The coupling constants $J_{i_1 \dots i_q}$ in Eq. (2.2) are Gaussian random variables with zero mean and variance

$$\langle J_{i_1 i_2 \dots i_q}^2 \rangle_J = \frac{(q-1)! J^2}{N^{q-1}} \frac{1}{p}, \quad (2.5)$$

where the factor p in the denominator compensates for the dependence of the average energy on p . The spectral statistics of the sparse SYK model with $q = 4$ have been discussed in [52, 56]. For sufficiently large k , the sparse SYK model can be classified into GOE, GSE, and GUE as in the original SYK model. However, for small values of k or k_{cpl} , the energy gap ratio is about 0.386 [56], indicating that the energy level spacing distribution of the sparse SYK model follows the Poisson distribution [62].

The Majorana fermions in the SYK model can be expressed as a spin chain using the Jordan-Wigner transformation. The convention used in this paper is

$$\psi_{2i-1} = \underbrace{\sigma_z \otimes \cdots \otimes \sigma_z}_{i-1} \otimes \sigma_x \otimes \underbrace{I \otimes \cdots \otimes I}_{\frac{N}{2}-i}, \quad (2.6)$$

$$\psi_{2i} = \underbrace{\sigma_z \otimes \cdots \otimes \sigma_z}_{i-1} \otimes \sigma_y \otimes \underbrace{I \otimes \cdots \otimes I}_{\frac{N}{2}-i}, \quad (2.7)$$

where $i = 1, \dots, \frac{N}{2}$ with N the number of Majorana fermions in consideration. In this basis, the Majorana fermions are viewed as a non-local object. In this paper, the partial trace/transpose operations are applied to a subset of qubits in this basis when computing the pseudo entropy and negativity numerically. One potential problem of this choice is the difficulty in physically interpreting such operations in the original Majorana fermion basis.

An alternative SYK-like model was recently proposed by formulating a randomly coupled model using qubits instead of fermions and it is called the SpinXY₄ model [63]. It closely resembles and demonstrates the chaotic behaviors of the SYK model. The SpinXY₄ model Hamiltonian with $\frac{N_{\text{Maj}}}{2}$ qubits, where N_{Maj} is the number of Majorana fermion which gives the same Hilbert space dimension, is given by

$$H_{\text{Spin}} = \sqrt{\frac{6}{N_{\text{Maj}}^3}} \sum_{1 \leq a < b < c < d \leq N_{\text{Maj}}} J_{abcd} i^{\eta_{abcd}} \mathcal{O}_a \mathcal{O}_b \mathcal{O}_c \mathcal{O}_d, \quad (2.8)$$

where the spin operators \mathcal{O} are

$$\mathcal{O}_{2i-1} = \underbrace{I \otimes \cdots \otimes I}_{i-1} \otimes \sigma_x \otimes \underbrace{I \otimes \cdots \otimes I}_{\frac{N}{2}-i}, \quad (2.9)$$

$$\mathcal{O}_{2i} = \underbrace{I \otimes \cdots \otimes I}_{i-1} \otimes \sigma_y \otimes \underbrace{I \otimes \cdots \otimes I}_{\frac{N}{2}-i}. \quad (2.10)$$

The coupling constants follow a probability distribution

$$P(J_{abcd}) = \frac{1}{\sqrt{2\pi}} e^{-J_{abcd}^2/2}, \quad (2.11)$$

which corresponds to zero mean and a variance of unity with this choice of scaling. The extra factor of $i^{\eta_{abcd}}$ comes from the fact that the \mathcal{O}_i operators are effectively a Pauli operator at a single site (qubit). Due to the algebra of the Pauli operators, if both $\mathcal{O}_{2i-1}\mathcal{O}_{2i}$ appear in a single term of the Hamiltonian. The Hamiltonian will no longer be Hermitian unless a factor of i is inserted by hand. The factor η_{abcd} is defined such that the Hermiticity of the Hamiltonian recovered. It counts the number of $\mathcal{O}_{2i-1}\mathcal{O}_{2i}$ pairs in the term e.g.

$\eta_{1237} = 1$ with $\mathcal{O}_1\mathcal{O}_2$ as a pair and $\eta_{1256} = 2$ with $\mathcal{O}_1\mathcal{O}_2$ and $\mathcal{O}_5\mathcal{O}_6$ as two pairs. One advantage of this model is that these operators are local in the spin basis and as a result, the partial trace/transpose operations are better physically interpreted. We will also use this model as an example of a chaotic system to study the properties of pseudo-entropy and negativity of entanglement in this paper.

3 Pseudo-entropy as a probe of chaos

3.1 Chaotic spectrum via pseudo-entropy

The spectral information of a disordered system is captured in the spectral form factor (SFF, denoted as $g(t, \beta)$). It is given by [28, 29, 64]

$$g(t, \beta) = \frac{\langle Z(\beta + it)Z^*(\beta + it) \rangle_J}{\langle Z(\beta) \rangle_J^2}, \quad (3.1)$$

where $Z(\beta + it) = \text{tr} e^{-(\beta + it)H}$ is the partition function with a complex temperature. It is sometimes more useful to subtract the disconnected pieces, $g_d(t, \beta)$, of the SFF to review the true correlation of the spectrum. The resulting quantity is the connected SFF, $g_c(t, \beta)$, given by

$$g_d(t, \beta) = \frac{\langle Z(\beta + it) \rangle_J \cdot \langle Z^*(\beta + it) \rangle_J}{\langle Z(\beta) \rangle_J^2}, \quad (3.2)$$

$$g_c(t, \beta) = g(t, \beta) - g_d(t, \beta). \quad (3.3)$$

At infinite temperature, the late time behavior of the SFF, $g(t, 0)$, is solely determined by the symmetry of the theory [29].

To review spectral information captured in pseudo-entropy, we consider a two-sided model with two uncoupled SYK models. We consider the transition matrix connecting the following two states

$$\begin{aligned} |\psi\rangle &= \frac{1}{Z(\beta)^{1/2}} \sum_n e^{-\frac{\beta}{4}(H_L + H_R)} |n_L\rangle \otimes |n_R\rangle, \\ |\varphi\rangle &= e^{\frac{it}{2}(H_L + H_R)} |\psi\rangle, \end{aligned} \quad (3.4)$$

where $|\psi\rangle$ is the thermofield double state (TFD). The TFD state can be understood as the canonical purification of the thermal density matrix of one of the two SYK models. The state $|\varphi\rangle$ can be interpreted as a one-sided time evolution of the TFD state. To compute the pseudo-entropy, we first construct the transition matrix

$$\mathcal{T}^{\psi|\varphi} = \frac{|\psi\rangle\langle\varphi|}{\langle\varphi|\psi\rangle}, \quad (3.5)$$

and then the reduced transition matrix of the R system is obtained by partial tracing over the L system

$$\mathcal{T}_R^{\psi|\varphi} = \text{tr}_L \mathcal{T}^{\psi|\varphi} = \frac{e^{-(\beta+it)H_R}}{Z(\beta+it)}. \quad (3.6)$$

Note that the reduced transition matrix resembles closely to the thermal density matrix of a single SYK model with a complex temperature $\beta+it$. Substituting this reduced transition matrix to the pseudo-entropy formula and taking the real part, we obtain

$$\begin{aligned} \text{Re}[S(\mathcal{T}_R^{\psi|\varphi})] &= -\text{Re} \left[\left\langle \text{tr}_R \mathcal{T}_R^{\psi|\varphi} \log \mathcal{T}_R^{\psi|\varphi} \right\rangle_J \right] \\ &= \langle \text{Re} [(\beta+it)\langle H_R \rangle_{\beta+it}] \rangle_J + \frac{1}{2} \left\langle \log \left(|Z(\beta+it)|^2 \right) \right\rangle_J. \end{aligned} \quad (3.7)$$

Here $\langle \dots \rangle_J$ denotes the disorder averaging. This result has been previously discussed in the CFT₂ case [49]. For the case of CFT₂, the first term can be evaluated explicitly and is proportional to $\frac{\beta}{\beta^2+t^2}$. Therefore, this term tends to zero at late times and vanishes exactly when $\beta = 0$. As a result, for the pseudo-entropy to be a proper chaos diagnostic quantity, we expect that the chaos signal at the late time or infinite temperature of a chaotic system should be contained in the last term. Without the disorder average, the last term in Eq. (3.7) is the logarithm of the spectral form factor (3.1) without the normalization. In the infinite temperature limit, the normalization coefficient $Z(0)^2$ in Eq. (3.3) is universal. It depends only on the Hilbert space dimension and is given by 2^N in the case of the SYK model. So without the disorder average, this term is equal to the logarithm of the spectral form factor up to an additive constant.

To relate the pseudo-entropy in Eq. (3.7) and the SFF, we need to express $\langle \log |Z|^2 \rangle_J$ as a function of $\langle |Z|^2 \rangle_J$, but computing the analytical expression of this function is challenging. We numerically calculate the n -th pseudo-Rényi entropy, $\langle \log |Z|^2 \rangle_J$ and $\log \langle |Z|^2 \rangle_J$, for different N , and then present the results in Figure 1. The reason we present pseudo-Rényi entropy instead of pseudo-entropy in Figure 1 will be explained below. We observe that as N increases, these three quantities gradually converge to the same value. Thus, we assume that for large but finite N , we can approximately represent the SFF by the second term of Eq. (3.7). A more elaborate examination is to check whether pseudo-Rényi entropy can exhibit information about the degeneracy of the system. We will discuss this issue in the following paragraph.

We present the numerical results of the real part of the pseudo-entropy of the SYK₄ model in Figure 2a. From Figure 2a, it can be observed that the pattern of the real part

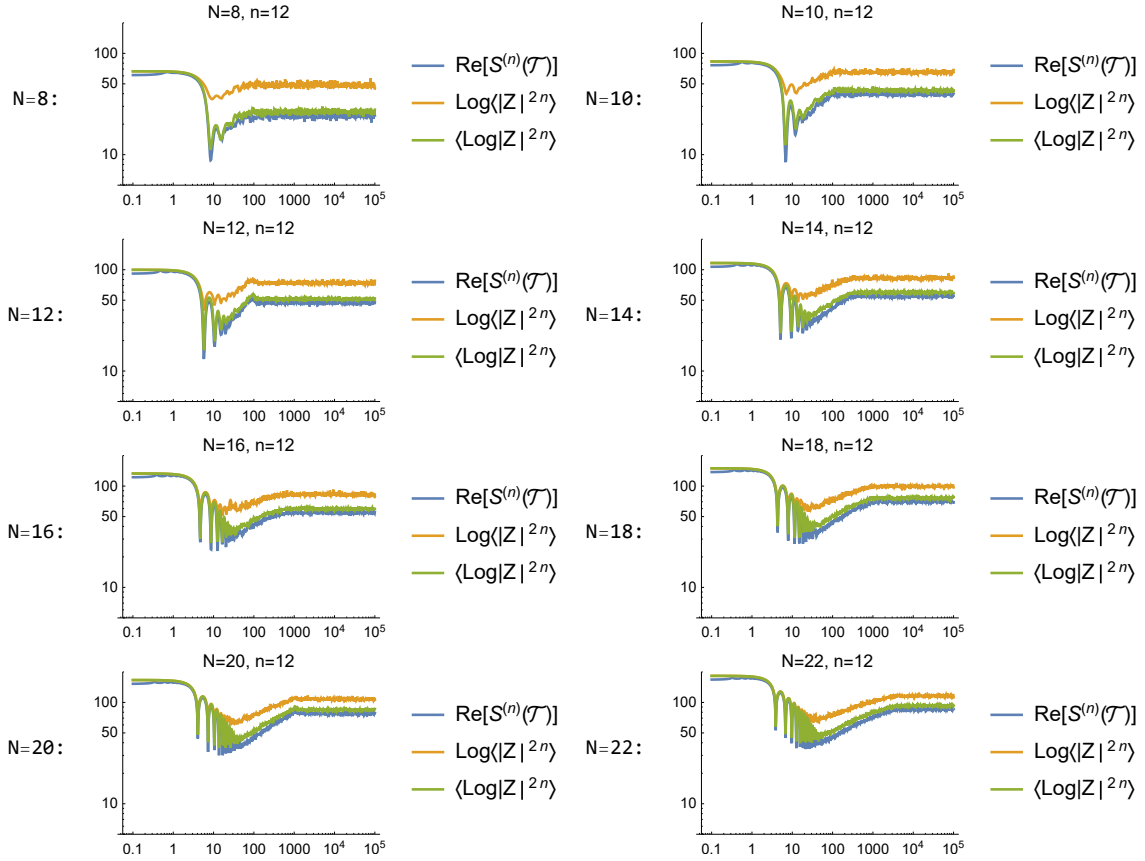


Figure 1: The comparison of $\text{Re}[S^{(n)}(\mathcal{T})]$, $\log \langle |Z|^n \rangle_J$, and $\langle \log |Z|^n \rangle_J$ with different values of N .

of the pseudo-entropy deviates from the standard results of the SFF. This deviation arises from the average of the Hamiltonian H_R in Eq. (3.7). To illustrate this, we display the first term and the total value of Eq. (3.7) in Figure 2b. The blue curve represents the real part of the pseudo-entropy $\text{Re}[S(\mathcal{T}_R^{\psi|\varphi})]$, while the yellow curve represents the first term in Eq. (3.7). It is evident that in the ramp and plateau regions, the average of the Hamiltonian dominates the behavior of $\text{Re}[S(\mathcal{T}_R^{\psi|\varphi})]$.

The pseudo-entropy may not be capable of fully characterizing the spectral form factor (SFF); however, we can utilize the n -th pseudo-Rényi entropy to depict the n -point function of the partition function. The real part of the n -th pseudo-Rényi entropy of the transition

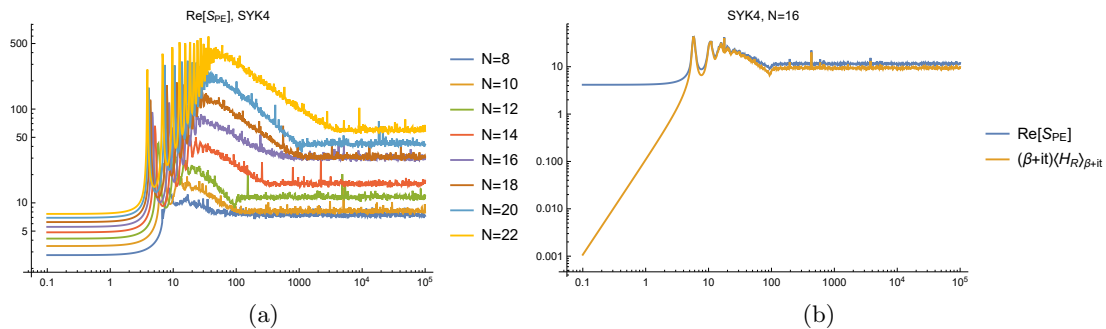


Figure 2: (a). The plot of the real part of the pseudo-entropy of the SYK₄ model with various values of N . (b). The blue curve is the real part of the pseudo-entropy $\text{Re}[S(\mathcal{T}_R^{\psi|\varphi})]$. The yellow curve is the first term in Eq. (3.7). One can find that, in the ramp and plateau region, the average of the Hamiltonian dominates the behavior of $\text{Re}[S(\mathcal{T}_R^{\psi|\varphi})]$.

matrix $\mathcal{T}_R^{\psi|\varphi}$ is given by

$$\begin{aligned} \text{Re} \left[S^{(n)}(\mathcal{T}_R^{\psi|\varphi}) \right] &= \left\langle \frac{1}{1-n} \text{Re} \left[\log \text{Tr} \left(\mathcal{T}_R^{\psi|\varphi} \right)^n \right] \right\rangle_J \\ &= \frac{1}{2(1-n)} \left(\left\langle \log |Z(n(\beta + it))|^2 \right\rangle_J - \left\langle \log |Z(\beta + it)|^{2n} \right\rangle_J \right). \end{aligned} \quad (3.8)$$

Note that the two terms in the parenthesis are not normalized, making the second term dominant in the real part of the pseudo-Rényi entropy for $n \gg 2$. In Figure 3, we present the real part of the n -th pseudo-Rényi entropy, $\log \langle |Z(\beta + it)|^{2n} \rangle_J$, and $\langle \log |Z(\beta + it)|^{2n} \rangle_J$ with various values of n . We observe that the curves of the n -th pseudo-Rényi entropy approach the curves of $\langle \log |Z(\beta + it)|^{2n} \rangle_J$ as n increases. We present our numerical results of $\text{Re} \left[S^{(n)}(\mathcal{T}_R^{\psi|\varphi}) \right]$ in Figure 4a. For comparison, we also display the logarithm of the n -point function in Figure 4b. Interestingly, we observe that the time scales t_d and t_p are the same for all n , which aligns with the result in Ref. [29].

In Figure 5, we present the pseudo-Rényi entropy for various values of N . To characterize the degeneracy of the models, we include the pseudo-Rényi entropy of the SYK model with N Majorana fermions multiplied by the normalization constant $(n-1)N$. The modified expression is given by

$$2(1-n)\text{Re} \left[S^{(n)}(\mathcal{T}_R^{\psi|\varphi}) \right] + (n-1)N = \left\langle \log \frac{|Z(int)|^2}{d_N^2} \right\rangle_J - \left\langle \log \frac{|Z(it)|^{2n}}{d_N^{2n}} \right\rangle_J, \quad (3.9)$$

where $d_N = 2^{N/2} = Z(0)$ represents the dimension of the Hilbert space of the SYK model with N Majorana fermions. The negative logarithmic term in Eq. (3.9) contributes to

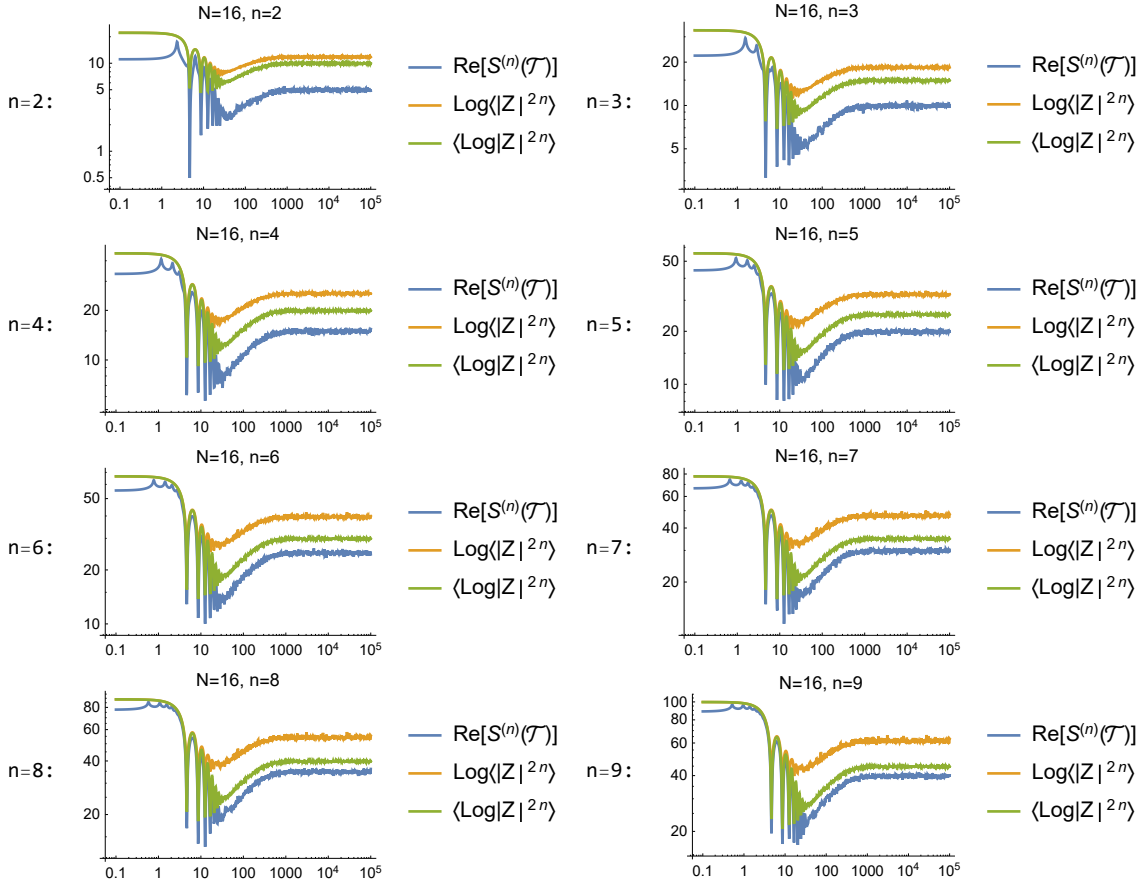


Figure 3: The comparison of $\text{Re}[S^{(n)}\mathcal{T}]$, $\log\langle|Z|^{2n}\rangle_J$, and $\langle\log|Z|^{2n}\rangle_J$ with different values of n .

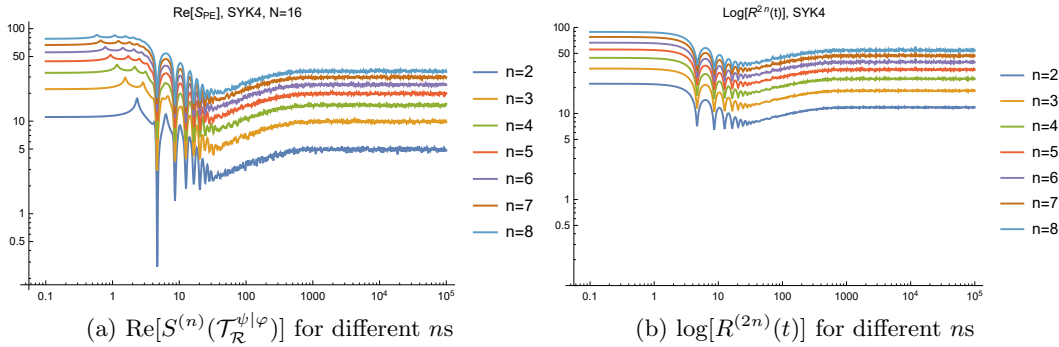


Figure 4: (a). The real part of the n -th pseudo-Rényi entropy. (b). Logarithm of $R_{2n}(t)$. $N = 16$, $n = 2, \dots, 8$.

the growth behavior in the slope region and the decay behavior in the ramp region. Furthermore, for large N ($N \geq 20$), we observe that the behaviors in the plateau region

approximately reflect the double degeneracy of the SYK model with $N \bmod 8 = 2, 4, 6$, while being nondegenerate for $N \bmod 8 = 0$. Conversely, for smaller values of N , significant deviations between $S^{(n)}(\mathcal{T})$ and $\log \langle |Z|^n \rangle$ disrupt the characterization of energy level degeneracy through the plateau behavior.

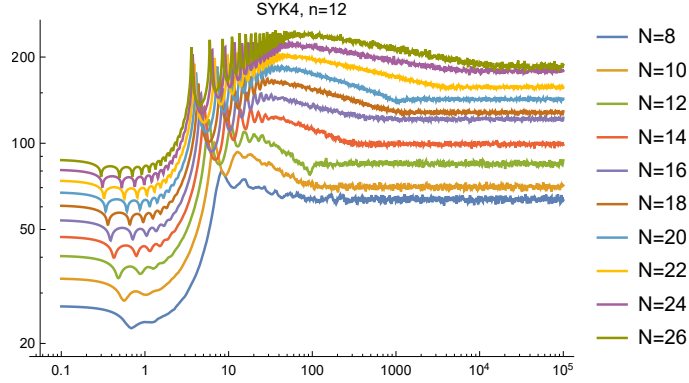


Figure 5: Plot of $2(1-n)\text{Re} \left[S^{(n)}(\mathcal{T}_R^{\psi|\varphi}) \right] + (n-1)N$ for various values of N .

3.2 Pseudo-entropy in the subsystem

In Section 3.1, we established that the real part of the pseudo-entropy for $\mathcal{T}_R^{\psi|\varphi}$ characterizes the properties of the spectral form factor. In this section, we focus on the pseudo-entropy of a subregion of the R system. Specifically, for the SYK model, we select the first several Majorana fermions of the R system as \bar{A} and then trace over \bar{A} to obtain the reduced transition matrix of A

$$\mathcal{T}_A^{\psi|\varphi} = \text{tr}_{\bar{A}} \mathcal{T}_R^{\psi|\varphi}. \quad (3.10)$$

By employing the Jordan-Wigner transformation, the state of the SYK model can be expressed in the particle number representation as follows

$$|\Psi\rangle = \sum_{n_1, \dots, n_{N/2}=0}^1 c_{n_1, \dots, n_{N/2}} |n_1, n_2, \dots, n_{N/2}\rangle, \quad (3.11)$$

where n_i represents the particle number of the i -th Dirac fermion in the state $|\Psi\rangle$. The eigenstate of the Hamiltonian on this basis can be decomposed as

$$\begin{aligned} |E_n\rangle &= \sum_{n_1, \dots, n_{N/2}=0}^1 \langle n_1, \dots, n_{N/2} | E_n \rangle |n_1, \dots, n_{N/2}\rangle \\ &= \sum_i \psi_i^n |i\rangle \end{aligned} \quad (3.12)$$

where we collectively represent the index $\{n_1, \dots, n_{N/2}\}$ by i for visual clarify and ψ_i^n is the wavefunction of the n -th energy eigenstate in this basis. We consider a subset A of the right system and trace out its complementary set $\bar{A} \cup L$. We label the quantities in subsystem A and \bar{A} by N and M respectively. The reduced transition matrix $\mathcal{T}_A^{\psi|\varphi}$ of $\mathcal{T}^{\psi|\varphi}$ is

$$\begin{aligned} \mathcal{T}_A^{\psi|\varphi} &= \text{tr}_{\bar{A}, L} \mathcal{T}^{\psi|\varphi} \\ &= \frac{1}{Z(\beta + it)} \sum_{\vec{N}_1, \vec{N}_2} \sum_{\vec{M}} \left(\langle \vec{M}, \vec{N}_1 | e^{-(\beta+it)H} | \vec{M}, \vec{N}_2 \rangle \right) | \vec{N}_1 \rangle \langle \vec{N}_2 |, \end{aligned} \quad (3.13)$$

where the vector \vec{N}/\vec{M} labels the eigenstates of the subsystem A or \bar{A} in the particle number basis. By using Eq. (3.12), we can express the Eq. (3.13) as

$$\mathcal{T}_A^{\psi|\varphi} = \frac{1}{Z(\beta + it)} \sum_{\vec{N}_1, \vec{N}_2} \sum_{\vec{M}} \sum_n (\psi_{\vec{M}\vec{N}_1}^n)^* (\psi_{\vec{M}\vec{N}_2}^n) e^{-(\beta+it)E_n} | \vec{N}_1 \rangle \langle \vec{N}_2 |. \quad (3.14)$$

The SYK model's spectral statistics can be approximated using the Random Matrix Theory (RMT) approach, as studied in works such as [29] and [28]. For example, in the case of the Gaussian Unitary Ensemble (GUE), the spectrum statistics are invariant under unitary conjugation, leading to the following expression for the density of states

$$dH = C |\Delta(\lambda)|^2 \prod_i d\lambda_i dU, \quad (3.15)$$

where $\Delta(\lambda)$ is the Vandermonde determinant and dU is the Haar measure of the unitary group U . The information of the eigenvector $\psi_{\vec{M}\vec{N}}^n$ are encoded in the unitary group U . So we can regard the eigenvalues E_n and eigenvector $\psi_{\vec{M}\vec{N}}^n$ of the Hamiltonian H as independent random variables. The Haar integral of the matrix elements of the unitary group element U satisfies [64–66]

$$\int dU U^j_k U^{\dagger l}_m = \frac{1}{L} \delta_m^j \delta_k^l, \quad (3.16)$$

where L is the dimension of the random matrix. Based on this relation, the disorder average of the Rényi entropy of the reduced transition matrix (3.14) is computable. We will estimate the real part of the pseudo-Rényi entropy of the SYK model's subsystem using the RMT formula in the large- L limit. Subsequently, we will complement our analysis by numerically calculating the pseudo-Rényi entropy for the SYK model using the exact diagonalization method.

The real part of the second pseudo-Rényi entropy is

$$\begin{aligned}
& - \left\langle \text{Re} \log \text{tr} \left(\mathcal{T}_A^{\psi|\varphi} \right)^2 \right\rangle_J = -\frac{1}{2} \left\langle \log \left| \text{tr} \left(\mathcal{T}_A^{\psi|\varphi} \right)^2 \right|^2 \right\rangle_J \\
& = -\frac{1}{2} \left\langle \log \left[\sum_{\vec{N}_1, \vec{N}_2} \sum_{\vec{M}_1, \vec{M}_2} \sum_{n_1, n_2} \left(\psi_{\vec{M}_1 \vec{N}_1}^{n_1} \right)^* \left(\psi_{\vec{M}_1 \vec{N}_2}^{n_1} \right) \left(\psi_{\vec{M}_2 \vec{N}_2}^{n_2} \right)^* \left(\psi_{\vec{M}_2 \vec{N}_1}^{n_2} \right) e^{-(\beta+it)(E_{n_1}+E_{n_2})} \right. \right. \\
& \quad \times \left. \left. \sum_{\vec{N}_3, \vec{N}_4} \sum_{\vec{M}_3, \vec{M}_4} \sum_{n_3, n_4} \left(\psi_{\vec{M}_3 \vec{N}_3}^{n_3} \right) \left(\psi_{\vec{M}_3 \vec{N}_4}^{n_3} \right)^* \left(\psi_{\vec{M}_4 \vec{N}_4}^{n_4} \right) \left(\psi_{\vec{M}_4 \vec{N}_3}^{n_4} \right)^* e^{-(\beta-it)(E_{n_3}+E_{n_4})} \right] \right\rangle_J \\
& + \frac{1}{2} \left\langle \log |Z(it)|^4 \right\rangle_J. \tag{3.17}
\end{aligned}$$

Upto this step, we also need to address the ensemble average of the logarithmic function of $|Z|$. Based on the implications of the numerical results in Section 3.1, we assume that the logarithm of $\langle |Z|^2 \rangle$ is well approximated by the average of $\log |Z|^2$ in the large system size limit. Therefore, the second term becomes the logarithm of a $2n$ -point function. Now let's temporarily disregard the logarithmic function and take $n = 2$ to calculate the expression

$$\begin{aligned}
& \sum_{\{\vec{N}_i\}} \sum_{\{\vec{M}_i\}} \sum_{\{n_i\}} \left\langle \left(\psi_{\vec{M}_1 \vec{N}_1}^{n_1} \right)^* \left(\psi_{\vec{M}_1 \vec{N}_2}^{n_1} \right) \left(\psi_{\vec{M}_2 \vec{N}_2}^{n_2} \right)^* \left(\psi_{\vec{M}_2 \vec{N}_1}^{n_2} \right) \right. \\
& \quad \left. \left(\psi_{\vec{M}_3 \vec{N}_3}^{n_3} \right) \left(\psi_{\vec{M}_3 \vec{N}_4}^{n_3} \right)^* \left(\psi_{\vec{M}_4 \vec{N}_4}^{n_4} \right) \left(\psi_{\vec{M}_4 \vec{N}_3}^{n_4} \right)^* e^{-i(E_{n_1}+E_{n_2}-E_{n_3}-E_{n_4})t} \right\rangle_J. \tag{3.18}
\end{aligned}$$

In Eq. (3.18), the disorder average of the wavefunctions and the eigenvalues can be taken independently. To calculate Eq. (3.18) more systematically, one can use a diagrammatic approach introduced in [67] and reviewed in appendix A. After taking the disorder average of the wavefunction, its time dependent part are the following three terms

$$\begin{aligned}
& \begin{array}{cc} \text{Diagram 1} & \text{Diagram 2} \end{array} = \frac{d_N^4 d_M^2}{d^4} |Z(2it)|^2 \tag{3.19}
\end{aligned}$$

$$\begin{aligned}
& \begin{array}{cc} \text{Diagram 3} & \text{Diagram 4} \end{array} = \frac{d_N^3 d_M^3}{d^4} Z(it)^2 Z(-2it) \tag{3.20}
\end{aligned}$$

$$\begin{aligned}
& \begin{array}{cc} \text{Diagram 5} & \text{Diagram 6} \end{array} = \frac{d_N^2 d_M^4}{d^4} |Z(it)|^4 \tag{3.21}
\end{aligned}$$

where $d = d_N d_M$ is the dimension of the Hilbert space of the total system, d_N is the dimension of the Hilbert space of subsystem A and d_M is the dimension of the Hilbert space of subsystem \bar{A} . In the above diagrams, solid lines and dashed lines represent subsystem A and its complement \bar{A} , respectively. In the left three diagrams, each circle represents a factor of $e^{iE_n t}$, while in the right three diagrams, since the matrix elements need to be

complex conjugated, each circle represents a factor of $e^{-iE_n t}$. Adding these three terms together, the final result of Eq. (3.18) is

$$\text{Eq. (3.18)} = \frac{1}{d^4} (d_N^2 d_M^4 |Z(it)|^4 + d_N^4 d_M^2 |Z(2it)|^2 + 2d_N^3 d_M^3 \text{Re} [Z(2it)Z(-it)^2]) . \quad (3.22)$$

Notice that $|Z(it)|^4$, $|Z(2it)|^2$ and $Z(2it)Z(-it)^2$ are unnormalized, so their magnitudes are of order $d^4 = d_N^4 d_M^4$, $d^2 = d_N^2 d_M^2$ and $d^3 = d_N^3 d_M^3$ respectively. Taking into account the factors in front of the each term, the magnitude are of order $d_N^6 d_M^8$, $d_N^6 d_M^4$ and $d_N^6 d_M^6$. When the dimension of M is sufficiently large, the first term in the parentheses dominates. In this case, the time-dependent part of Eq. (3.18) and the second term of Eq. (3.17) are approximately equal. Therefore, the 2nd pseudo-Rényi entropy approximates to a constant. When d_M is relatively small, the magnitudes of the last two terms become comparable to that of the first term. In this case, the 2nd pseudo-Rényi entropy exhibits the characteristics of the SFF.

For the finite N system, we present the numerical results of the real part of the pseudo-Rényi entropy of the subsystem A in Figure 6 with various N and sizes of the subsystem A . In Figure 6a, we observe that when N_A is small, the 2nd pseudo-Rényi entropy changes over time small relatively. However, the similar property is not very evident in other figures. For the larger value of N_A , the results exhibit the slope-ramp-plateau characteristic observed in the SFF. This property is consistent with the result in Eq. (3.22).

After demonstrating the similarity between the pseudo-Rényi entropy of the reduced transition matrix and the SFF, we aim to conduct a more thorough examination of the pseudo-entropy's properties. As discussed in Section 2, the energy gap ratio of the sparse SYK model undergoes an integrable-chaotic transition as the parameter k_{cpl} increases [56]. In the ensuing paragraph, we delve into a numerical exploration of the pseudo-entropy of the sparse SYK model. The outcomes of our investigation are presented in Figure 7. Each figure showcases results for a fixed N and varying values of k_{cpl} . Across all figures, we discern a consistent pattern: a slope region emerges in the early times, followed by a ramp region during intermediate times, and culminating in a plateau region at later times. Moreover, the time scales t_d and t_p of the sparse SYK model with sufficiently large k_{cpl} closely approximate the values predicted by RMT. Conversely, for the sparse SYK model with lower k_{cpl} values, the time scales t_d and t_p are notably shorter than those of the dense SYK model. Thus, we can confidently conclude that the real part of the pseudo-entropy of the sparse SYK model exhibits an integrable-chaotic transition as the parameter k_{cpl} increases, aligning harmoniously with the findings in [56]. In Figure 8, we also exhibit

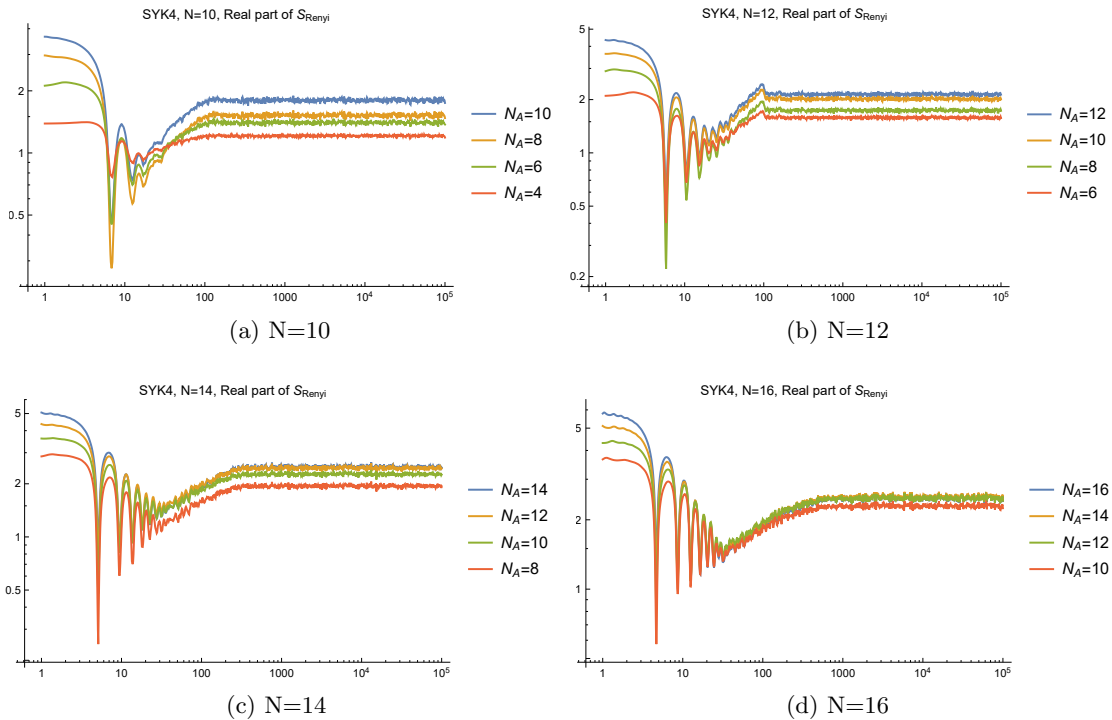


Figure 6: Plot of the real part of the pseudo-Rényi entropy of the SYK₄ model with various values of N .

the same quantities calculated by the sparse spinXY₄ model. We find that the results are consistent with those of the sparse SYK₄ model.

4 The local operator entanglement

In this section, we endeavor to extend the discussions put forth in [8, 15, 16], to establish a connection between the evolution of pseudo-entropy and the concept of scrambling. It is believed that the scrambling behavior of the evolution operator $U(t)$ can serve as a diagnostic tool for identifying the quantum chaotic properties of certain systems. Moreover, recent work by Dowling et al. [68] has proven that the linear growth behavior of the Rényi entropy is a necessary condition for quantum chaos.

The relationship between entanglement entropy and scrambling has been discussed in the Ref. [8, 15], where they demonstrated that the OTOC is equal to the negative exponential of the second Rényi entropy. In order to generalize the Rényi entropy to pseudo-Rényi entropy, we briefly review the derivation in [15]. Consider the 4-point correlation function $\sum_{M \in B} \text{Tr} [M(t) O e^{-\beta H} O^\dagger M(t) O e^{-\beta H} O^\dagger]$, where the operator M belongs to the subsystem

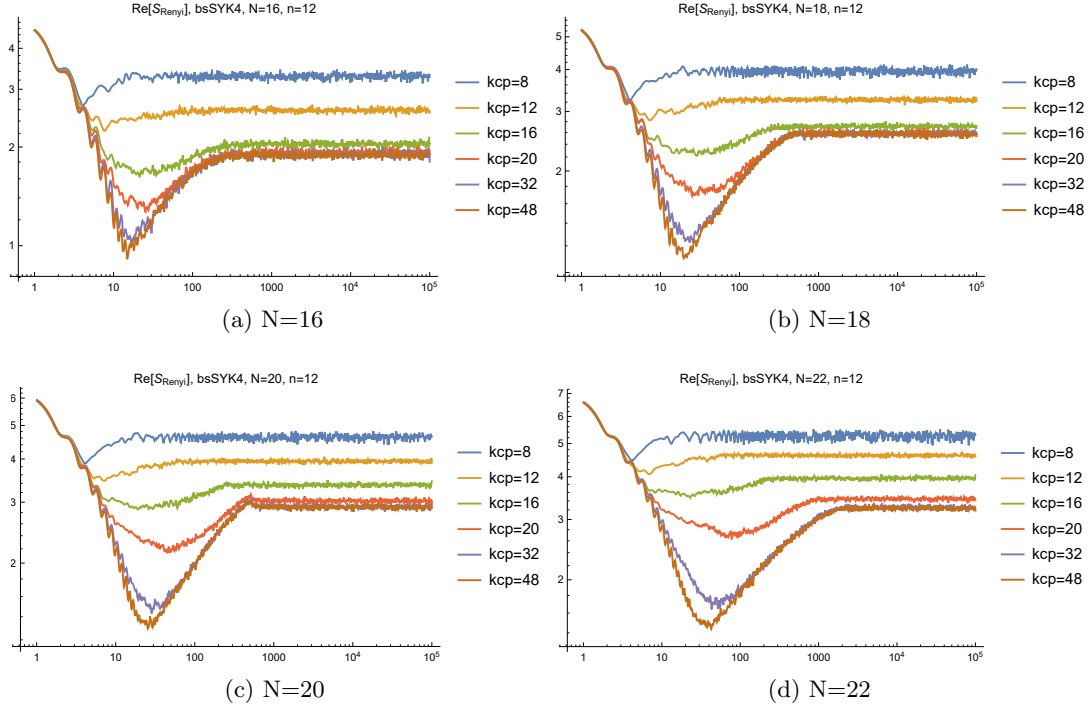


Figure 7: Real part of the pseudo-Rényi entropy of the binary sparse SYK model with different N and k_{cpl} .

B and satisfies $\sum_{M \in B} MOM = \text{Tr}_B O \otimes I$. Then, the above OTOC can be rewritten as $\text{Tr}_A [\text{Tr}_B [Oe^{-\beta H} O^\dagger] \text{Tr}_B [Oe^{-\beta H} O^\dagger]]$. In this case, we can define $\rho_A = \text{Tr}_B [Oe^{-\beta H} O^\dagger]$ and obtain the following relation

$$e^{-S_A^{(2)}} = \sum_{M \in B} \text{Tr} \left[M(t) O e^{-\beta H} O^\dagger M(t) O e^{-\beta H} O^\dagger \right]. \quad (4.1)$$

To generalize the Rényi entropy in the above formula to pseudo-Rényi entropy, we can naively replace the operator $Oe^{-\beta H} O^\dagger$ in the density matrix by $O_1(t_1) e^{-\beta H} O_2(t_2)$. In this case, we can construct the OTOC only by using O_1 and O_2 without M . Considering the normalization factor and purifying the density matrix $e^{-\beta H}$ by a auxiliary system L , the transition matrix in this case is

$$\mathcal{T} = \frac{O_1(t_1) |TFD\rangle \langle TFD| O_2^\dagger(t_2)}{\langle TFD| O_2^\dagger(t_2) O_1(t_1) |TFD\rangle}. \quad (4.2)$$

which is the transition matrix of the local quenched system [45, 47]. The reduced transition matrix of the system R is

$$\mathcal{T}_R = \text{Tr}_L \mathcal{T} = \frac{O_1(t_1) \rho O_2^\dagger(t_2)}{\text{Tr} \left[O_1(t_1) \rho O_2^\dagger(t_2) \right]}, \quad (4.3)$$

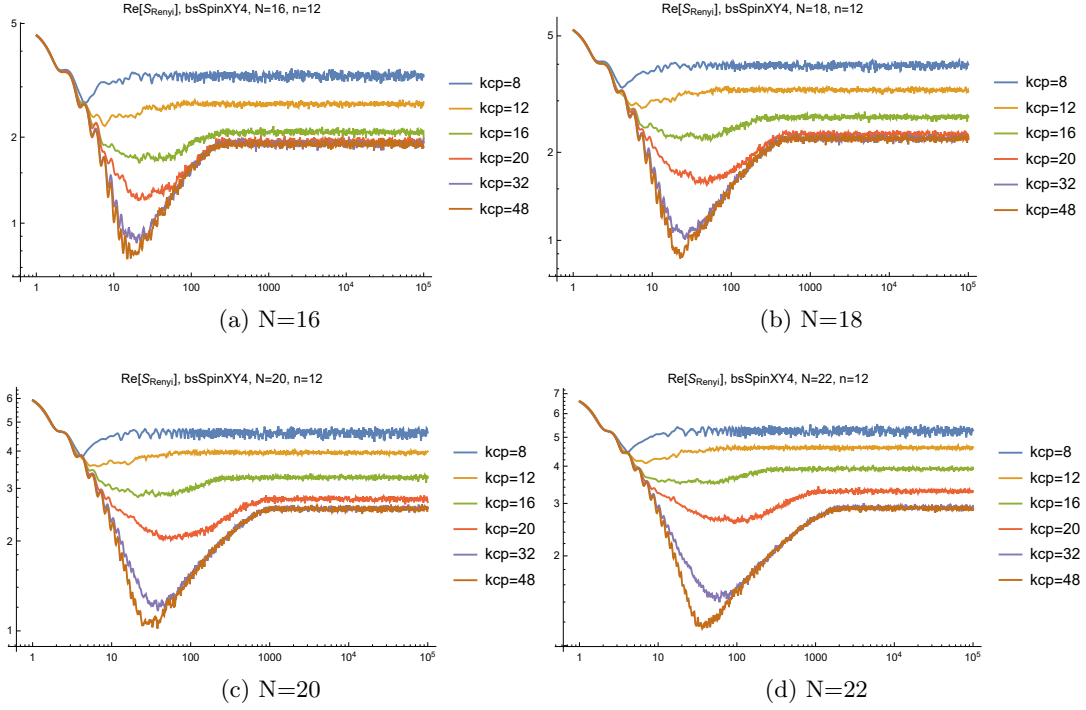


Figure 8: Real part of the pseudo-Rényi entropy of the binary sparse spinXY₄ model with different k_{cpl} .

where $\rho = e^{-\beta H} / \text{Tr}[e^{-\beta H}]$. The exponent of the second pseudo-Rényi entropy is

$$\text{Tr} \mathcal{T}_R^2 = \frac{\text{Tr} \left[O_1(t_1) \rho O_2^\dagger(t_2) O_1(t_1) \rho O_2^\dagger(t_2) \right]}{\text{Tr} \left[O_1(t_1) \rho O_2^\dagger(t_2) \right]^2} \quad (4.4)$$

In contrast to the traditional OTOC, the normalization factor in Eq. (4.4) is $\langle O_2^\dagger(t_2) O_1(t_1) \rangle_\beta^2$, which differs from $\langle O_1(\beta) O_1 \rangle_\beta \langle O_2(\beta) O_2 \rangle_\beta$. It is time-dependent and vanishes at leading order in the large N expansion. In the SYK model, to obtain a standard OTOC, we choose the operators O_1 and O_2 as follows

$$\begin{aligned} O_1 &= \psi_i(t) + \psi_j(t), \\ O_2 &= \psi_i(t) + \psi_j(0). \end{aligned} \quad (4.5)$$

At the leading order of N , the trace of \mathcal{T}_R^2 can be approximated by

$$\begin{aligned} \text{Tr} \mathcal{T}_R^2 &= \frac{\text{Tr} \left[O_1 \rho O_2^\dagger O_1 \rho O_2^\dagger \right]}{\text{Tr} \left[O_1 \rho O_2^\dagger \right]^2} \\ &= \frac{\text{Tr} \left[\rho^2 + \psi_i(t) \rho \psi_j(t) \psi_i(t) \rho \psi_j(t) \right] + 2 \text{Tr} \left[\psi_i(t) \rho \psi_j(0) \psi_i(t) \rho \psi_j(0) \right]}{\text{Tr} \left[\psi_i(t) \rho \psi_i(t) \right]^2} + O(N^{1-q}), \end{aligned} \quad (4.6)$$

where the first term in the numerator is time-independent and cancels out precisely when $\beta = 0$, while the second term corresponds to a standard OTOC. The infinite temperature OTOC of the SYK model has been obtained in [69]. Its expression is

$$F_{\text{OTOC}} = 1 - \frac{1}{2N} \cosh 2\mathcal{J}t. \quad (4.7)$$

The period of the exponential decay occurs between the scales $1/2\mathcal{J}$ and $1/2\mathcal{J} \log 2N$ approximately. At the leading order of the large N expansion, $e^{-2\langle S^{(2)} \rangle_J}$ can be approximated by $\langle e^{-2S^{(2)}} \rangle_J$ where $\langle A \rangle_J$ means the disorder average of A . In Figure 9, we provide numerical results for the second pseudo-Rényi entropy of the binary sparse SYK model and binary sparse SpinXY₄ model. In this figure, we choose $N = 16$ and $\mathcal{J} = 1/\sqrt{2}$, hence the period of exponential decay is approximately 0.7 to 2.5. As shown in Figure 9a and 9c, for larger values of k_{cpl} , there exists a region of linear growth of the second pseudo-Rényi entropy around the scrambling time, while for smaller k_{cpl} , this linear growth region is not as prominent. As a comparison, we provide the negative exponent of the second pseudo-Rényi entropy, i.e., OTOC in Eq. (4.6), in Figure 9b and 9d. For the SpinXY₄ model, the spin operators satisfy commutation relations rather than anti-commutation relations. Therefore, the first term in the numerator of Eq. (4.6) is not equal to 0, leading to a constant shift of 1 in Figure 9d. After ignoring this shift, the late-time limits of SYK₄ and SpinXY₄ both tend to be nonzero constants for the smaller values of k_{cpl} , which agrees with the results of Ising CFT obtained in Ref. [70].

5 Negativity of entanglement

This section discusses the negativity of entanglement as a probe of chaos in the binary sparse SYK model. We first review the definition of negativity and our set-up and present our numerical result.

The negativity [71–74] is considered as a measure of quantum entanglement for a mixed state. Given a density matrix ρ , the negativity, $\mathcal{N}(\rho)$, is computed as the trace norm of

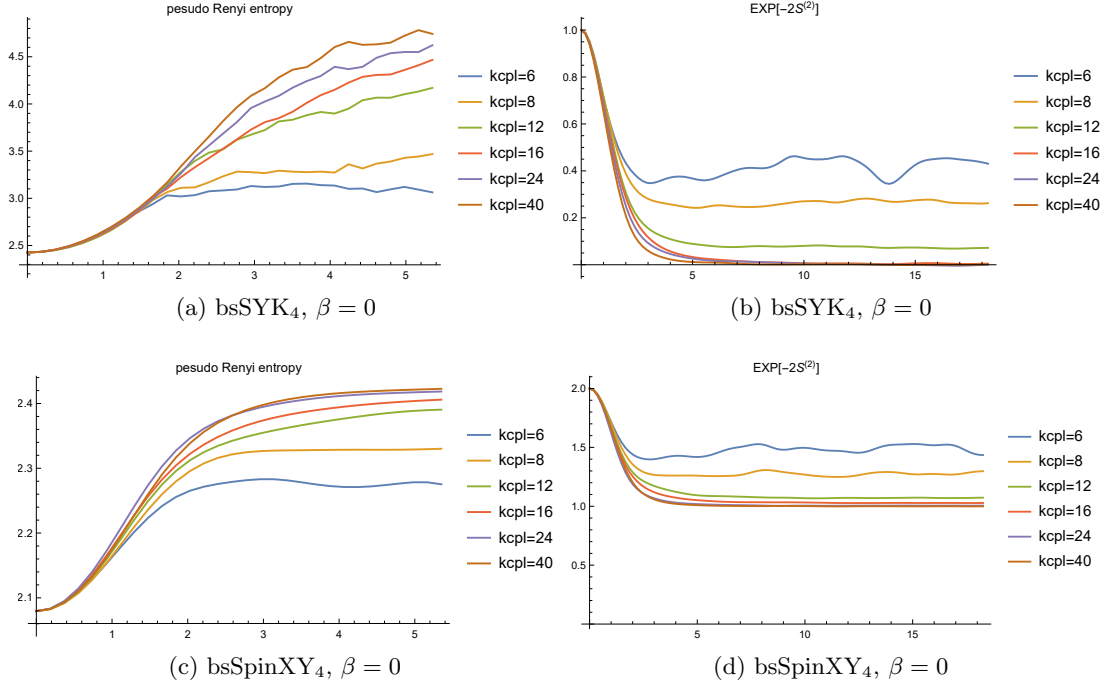


Figure 9: Plot of the 2nd pseudo-Rényi entropy of the binary sparse SYK₄ and SpinXY₄ model with various values of k_{cpl} .

the partial transposed density matrix.

$$\mathcal{N}(\rho) = \frac{1}{2} (\|\rho^{\Gamma_A}\|_1 - 1) , \quad (5.1)$$

where Γ_A denotes the (partial-) transpose operation on the subsystem A and $\|X\|_1 = \text{Tr}\sqrt{X^\dagger X}$ denotes the trace norm of the matrix X . To be more explicit, consider a total density matrix constructed from a tensor product of two Hilbert spaces $\mathcal{H}_A \otimes \mathcal{H}_B$, it can be expressed as

$$\rho = \sum_{ij,kl} c_{ij,kl} |i\rangle \langle j|_A \otimes |k\rangle \langle l|_B . \quad (5.2)$$

A partial transpose operation on the subsystem A is then

$$\rho^{\Gamma_A} = \sum_{ij,kl} c_{ij,kl} |j\rangle \langle i|_A \otimes |k\rangle \langle l|_B \quad (5.3)$$

$$= \sum_{i^*,j^*,kl} c_{j^*i^*,kl} |i^*\rangle \langle j^*|_A \otimes |k\rangle \langle l|_B . \quad (5.4)$$

Denoting the set of eigenvalues of the partial transposed density matrix as $\{\lambda_i\}$, then the

negativity is

$$\mathcal{N}(\rho) = \sum_i \frac{1}{2} (|\lambda_i| - \lambda_i), \quad (5.5)$$

which is the sum of all the negative eigenvalues of ρ^{Γ_A} .

5.1 Pseudo-negativity in binary sparse SYK₄

We consider the transition matrix constructed in the previous section which is just a single-sided time evolution of the thermal density matrix

$$\rho(\beta, t) = \sum_n e^{-(\beta+it)E_n} |n\rangle \langle n|, \quad (5.6)$$

where E_n is the energy of the eigenstate $|n\rangle$ of the Hamiltonian $\hat{H} |n\rangle = E_n |n\rangle$.

For the SYK model, we can use the spin-chain representation of the Majorana fermions in Eq. (2.6) and (2.7)

$$\begin{aligned} \psi_{2i-1} &= \sigma_3 \otimes \cdots \otimes \sigma_3 \otimes \sigma_1 \otimes \sigma_0 \otimes \cdots \otimes \sigma_0, \\ \psi_{2i} &= \sigma_3 \otimes \cdots \otimes \sigma_3 \otimes \sigma_2 \otimes \sigma_0 \otimes \cdots \otimes \sigma_0. \end{aligned} \quad (5.7)$$

Utilizing the properties of Pauli matrices, we have

$$\begin{cases} \sigma_2 \sigma_2 \sigma_2 = \sigma_2 = -\sigma_2^T \\ \sigma_2 \sigma_i \sigma_2 = -\sigma_i = -\sigma_i^T, \quad \text{for } i = 1, 3. \end{cases} \quad (5.8)$$

We introduce the unitary operator $U_i = \sigma_2$ acting on the i -th site and define $U_A = \prod_i U_i$ for $i \in A$. The partial transposition of the Majorana fermion can be obtained by $\psi_i^{TA} = (-1)^{\#(i)} U \psi_i U^\dagger$ where $\#(i)$ is the number of Pauli operators of ψ_i in the subsystem A . For the SYK model (2.1), the partial transposition of the Hamiltonian is given by

$$\begin{aligned} H_{\text{SYK}_4}^{TA} &= \sum_{i,j,k,l} J_{ijkl} (\psi_i \psi_j \psi_k \psi_l)^{TA} \\ &= U_A \left(\sum_{i,j,k,l} J_{ijkl} (-1)^{\#(i)+\#(j)+\#(k)+\#(l)} \psi_i \psi_j \psi_k \psi_l \right) U_A^\dagger \\ &:= U_A H'_{\text{SYK}_4} U_A^\dagger. \end{aligned} \quad (5.9)$$

Because the coupling constant is a Gaussian distribution with zero mean, we can absorb the factor $(-1)^{\#(i)+\#(j)+\#(k)+\#(l)}$ into J_{ijkl} and the distribution of the redefined coupling

constant is the same as the original one. As a result, we can express the pseudo-negativity of the SYK₄ model as

$$\begin{aligned}\mathcal{N} &= \frac{1}{2} \left(\text{Tr} \sqrt{\rho^{T_A \dagger} \rho^{T_A}} - 1 \right) = \frac{1}{2} \left(\text{Tr} \sqrt{\left(U_A \rho' U_A^\dagger \right)^\dagger U_A \rho' U_A^\dagger} - 1 \right) = \frac{1}{2} \left(\text{Tr} \sqrt{\rho'^\dagger \rho'} - 1 \right) \\ &= \frac{1}{2} \left[\left(\frac{\sqrt{Z(\beta + it) Z(\beta - it)}}{Z'(\beta)} \right)^{-1} - 1 \right]\end{aligned}\quad (5.10)$$

where $\rho' = e^{-\beta H'_{\text{SYK}_4}} / Z(\beta + it)$ and $Z(\beta \pm it)$ are the partition function defined by the original Hamiltonian. According to Eq. (5.10), one can easily find the relation between the pseudo-negativity and SFF. For the Pauli spinXY₄ model, the analysis presented earlier is similar and leads to the same results.

We numerically compute the negativity of this transition matrix and display our results in Figure 10. The left two figures are pseudo-negativity \mathcal{N} of SYK₄ model and SpinXY₄ model respectively and the right two figures are the ‘‘SFFs’’ expressed by \mathcal{N} by using Eq. (5.10). Further, we examine whether pseudo-negativity can capture signals of integrable-chaos transition and display our results in Figure 11. The results are consistent with the results in [52].

5.2 Diagrammatic computation

We can also derive the expression of pseudo-negativity Eq. (5.10) in the large system size regime using a diagrammatic technique. We extend the diagrammatic computation in [67] and keep only the leading order term. The starting point is the expression of the partially transposed transition matrix

$$\rho(t) = Z(\beta + it)^{-1} \sum_n e^{-(\beta + it)E_n} |n\rangle \langle n| \quad (5.11)$$

$$= Z(\beta + it)^{-1} \sum_n \sum_{ik,jl} e^{-(\beta + it)E_n} c_{ij}^n c_{kl}^{n*} |i\rangle \langle k|_A \otimes |j\rangle \langle l|_B \quad (5.12)$$

$$\rho^{T_B}(t) = Z(\beta + it)^{-1} \sum_n \sum_{ik,jl} e^{-(\beta + it)E_n} c_{ij}^n c_{kl}^{n*} |i\rangle \langle k|_A \otimes |l\rangle \langle j|_B. \quad (5.13)$$

Our strategy is to compute its norm using the replica trick and analytic continue the expression. The norm of the transition matrix is defined by

$$\|\rho^{T_B}(t)\| = \text{Tr} \sqrt{\rho^{T_B \dagger} \rho^{T_B}} \quad (5.14)$$

$$= |Z|^{-1} \text{Tr} \sqrt{\sum_{m,n} e^{-\beta(E_n + E_m)} e^{-i(E_n - E_m)t} c_{ij}^{*n} c_{kl}^n c_{il}^m c_{cd}^{*m} |k\rangle \langle c|_A \otimes |j\rangle \langle d|_B}, \quad (5.15)$$

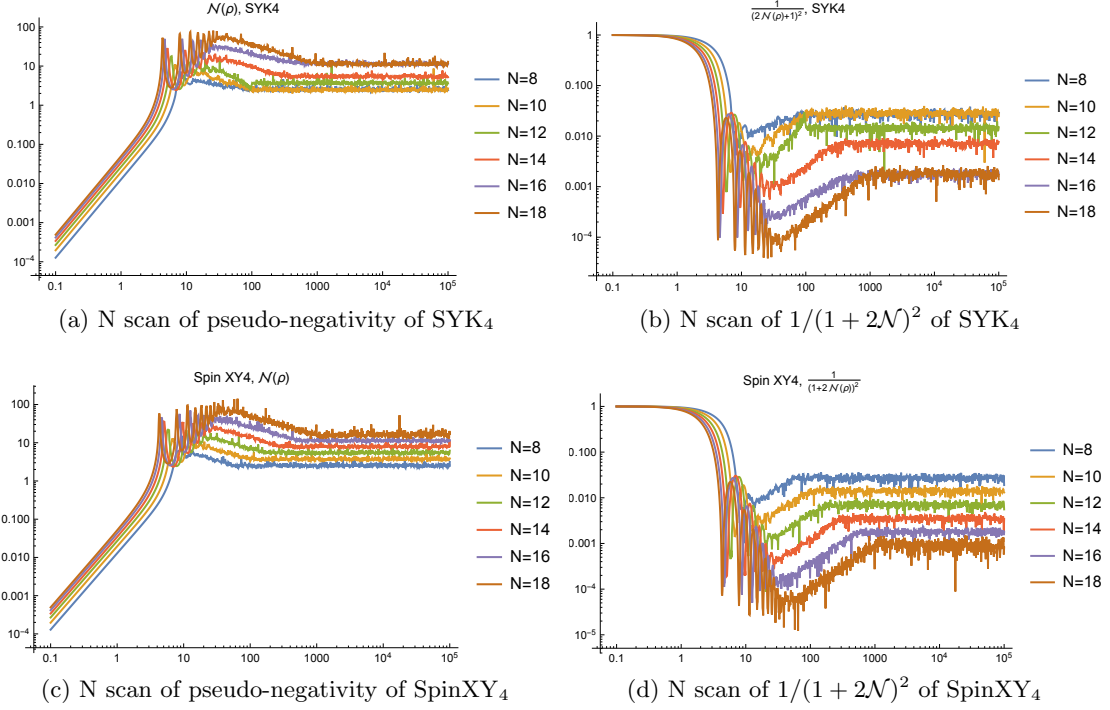


Figure 10: Results of pseudo-negativity of the SYK₄ and SpinXY₄ models with different N .

where $|Z| = |Z(\beta + it)|$. By using the replica trick, we consider the expression

$$\text{Tr}(\rho^{T_B^\dagger} \rho^{T_B})^n = |Z|^{-2n} \text{Tr} \left(\sum_{m,n} e^{-\beta(E_n + E_m)} e^{-i(E_n - E_m)t} c_{ij}^{*n} c_{kl}^n c_{il}^m c_{cd}^{*m} |k\rangle \langle c|_A \otimes |j\rangle \langle d|_B \right)^n, \quad (5.16)$$

To apply the diagrammatic technique, we re-express the equation in the following form

$$\text{Tr}(\rho^{T_B^\dagger} \rho^{T_B})^n \equiv \text{Tr} (M_{ij,ab})^n \quad (5.17)$$

$$= |Z|^{-2n} \text{Tr} \left(\sum_{I,J} e^{-\beta(E_I + E_J)} e^{-i(E_I - E_J)t} (d_{ia} d_{jb}^*)^{IJ} |ij\rangle \langle ab| \right)^n, \quad (5.18)$$

where we have defined $d_{ia} = c_{il}^I c_{al}^{J*}$ and its diagrammatic representation is in Fig.12b. Following [67], we compute the leading order contribution here. The technical detail is given in Appendix A. The leading order diagram is where all the transition matrices are connected by the averaging procedure as illustrated in Fig.12d.

The diagram contains n loops of subsystem A and B each and there are a total of n

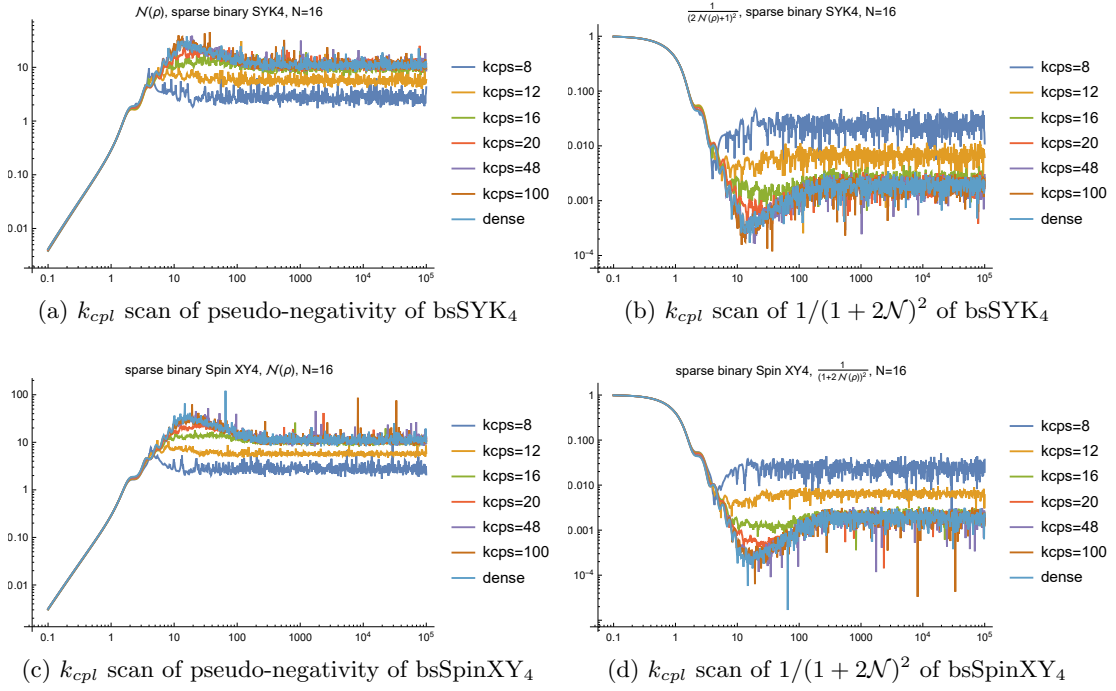


Figure 11: Results of pseudo-negativity of the binary sparse SYK₄ and SpinXY₄ models with different k_{cpl} .

averaging lines. Putting it together then we have

$$\text{Tr}M^n \approx |Z|^{-2n} \frac{1}{d^n} \times d_A^n \times d_B^n \times Z(2n\beta) \quad (5.19)$$

$$= |Z(\beta + it)|^{-2n} Z(2n\beta), \quad (5.20)$$

where we have used $d = d_A d_B$. Analytic continue this expression to $n \rightarrow \frac{1}{2}$, we have

$$\lim_{n \rightarrow \frac{1}{2}} \text{Tr}M^n \approx \frac{Z(\beta)}{\sqrt{Z(\beta + it)Z(\beta - it)}}. \quad (5.21)$$

Substituting it back to the expression of negativity, we then obtain

$$\mathcal{N} = \frac{1}{2} \left[\text{Tr} \sqrt{\rho^{T_B \dagger} \rho^{T_B}} - 1 \right] \quad (5.22)$$

$$\approx \frac{1}{2} \left[\frac{Z(\beta)}{\sqrt{Z(\beta + it)Z(\beta - it)}} - 1 \right], \quad (5.23)$$

which is a good approximation to pseudo-negativity.

6 Summary and prospect

In this paper, we investigate the possibility of probing the quantum chaotic behavior of a system through pseudo-entropy, an extension of entanglement entropy calculated using

the so-called transition matrix \mathcal{T} . Unlike the density matrix, the transition matrix can be defined using two non-orthogonal states $|\psi\rangle$ and $|\phi\rangle$, namely $\mathcal{T} = \frac{|\psi\rangle\langle\phi|}{\langle\phi|\psi\rangle}$. By choosing different states $|\psi\rangle$ and $|\phi\rangle$, one can establish connections between pseudo-entropy and various quantum mechanical quantities. In this work, we attempt to relate pseudo-entropy and pseudo-Rényi entropy to the SFF, OTOC, and entanglement negativity. We numerically compute the pseudo-entropy and pseudo-Rényi entropy of the SYK₄ model using exact diagonalization methods and find that these quantities exhibit similar characteristics to the corresponding SFF, OTOC, and entanglement negativity. To validate our proposal that pseudo-entropy and pseudo-Rényi entropy can indeed distinguish between chaotic and integrable systems, we calculate these quantities for the binary sparse SYK₄ model. By varying the pruning parameter k_{cpl} , we indeed observe an integrable-to-chaotic phase transition, consistent with existing research findings [53, 56, 70].

One advantage of the transition matrix is that it can be defined through the weak value of an operator, making it correspond to an observable [37]. Therefore, a natural choice for the states $|\psi\rangle$ and $|\phi\rangle$ is the initial state and final state of the system. In constructing the connection between pseudo-Rényi entropy and OTOCs, we chose a somewhat peculiar state that may not be readily realized by the physical evolution of another state. Therefore, we aim to find a more natural transition matrix to construct OTOCs. Additionally, we also aim to establish relationships between pseudo-entropy and other measures of quantum chaos, such as circuit complexity [75–77] or K-complexity [18, 19, 24], among others. Finally, we hope to utilize the holographic principle [35] to find the bulk gravitational dual of the transition matrix constructed in the previous sections and establish connections between the properties of pseudo-entropy and the chaotic behavior of black holes.

Acknowledgments

We would like to thank Zhuo-Yu Xian, Yu-Xuan Zhang, and Zi-Xuan Zhao for valuable discussions related to this work. S.H. also would like to appreciate the financial support from Jilin University and the Max Planck Partner group, as well as the Natural Science Foundation of China Grants No. 12075101, No. 12235016. P.H.C.L acknowledges the support from JSPS KAKENHI (Grant No. 20H01902 and JP23H01174), and MEXT KAKENHI (Grant No. 21H05462).

and the rule of the ensemble average of each pair of random variables becomes

$$\langle X_{ia}^m X_{bj}^{n*} \rangle = \frac{1}{d_{AdB}} \delta_{ij} \delta_{ab} \delta^{mn}. \quad (\text{A.8})$$

The other rules remain unchanged. With this diagrammatic technique, we evaluate Eq. (3.18) and obtain the result Eq. (3.22). The computation of pseudo-negativity follows similarly. Although the explicit forms of the matrix quantity that we need for the computation of pseudo-entropy and pseudo-negativity are different, the diagrammatic technique follows closely. We simply need to modify the interpretation of the coefficients (thermal factors) of the matrix quantity accordingly. Given the similarity, we simply summarize the diagrammatic rules for the pseudo-negativity in Figure 12. The matrix quantity of interest for pseudo-negativity is $M = \rho^{TB\dagger} \rho^{TB}$ defined by Eq. (5.17) instead of $\mathcal{T}_{ia,jb}$ in Eq. (A.6) for the pseudo-entropy above.

References

- [1] P. Hayden and J. Preskill, *Black holes as mirrors: Quantum information in random subsystems*, *JHEP* **09** (2007) 120, [[arXiv:0708.4025](#)].
- [2] Y. Sekino and L. Susskind, *Fast Scramblers*, *JHEP* **10** (2008) 065, [[arXiv:0808.2096](#)].
- [3] J. M. Maldacena, *The Large N limit of superconformal field theories and supergravity*, *Adv. Theor. Math. Phys.* **2** (1998) 231–252, [[hep-th/9711200](#)].
- [4] S. S. Gubser, I. R. Klebanov, and A. M. Polyakov, *Gauge theory correlators from noncritical string theory*, *Phys. Lett. B* **428** (1998) 105–114, [[hep-th/9802109](#)].
- [5] E. Witten, *Anti-de Sitter space and holography*, *Adv. Theor. Math. Phys.* **2** (1998) 253–291, [[hep-th/9802150](#)].
- [6] S. H. Shenker and D. Stanford, *Black holes and the butterfly effect*, *JHEP* **03** (2014) 067, [[arXiv:1306.0622](#)].
- [7] S. H. Shenker and D. Stanford, *Stringy effects in scrambling*, *JHEP* **05** (2015) 132, [[arXiv:1412.6087](#)].
- [8] P. Hosur, X.-L. Qi, D. A. Roberts, and B. Yoshida, *Chaos in quantum channels*, *JHEP* **02** (2016) 004, [[arXiv:1511.04021](#)].
- [9] M. Van Raamsdonk, *Building up spacetime with quantum entanglement*, *Gen. Rel. Grav.* **42** (2010) 2323–2329, [[arXiv:1005.3035](#)].
- [10] J. Maldacena and L. Susskind, *Cool horizons for entangled black holes*, *Fortsch. Phys.* **61** (2013) 781–811, [[arXiv:1306.0533](#)].

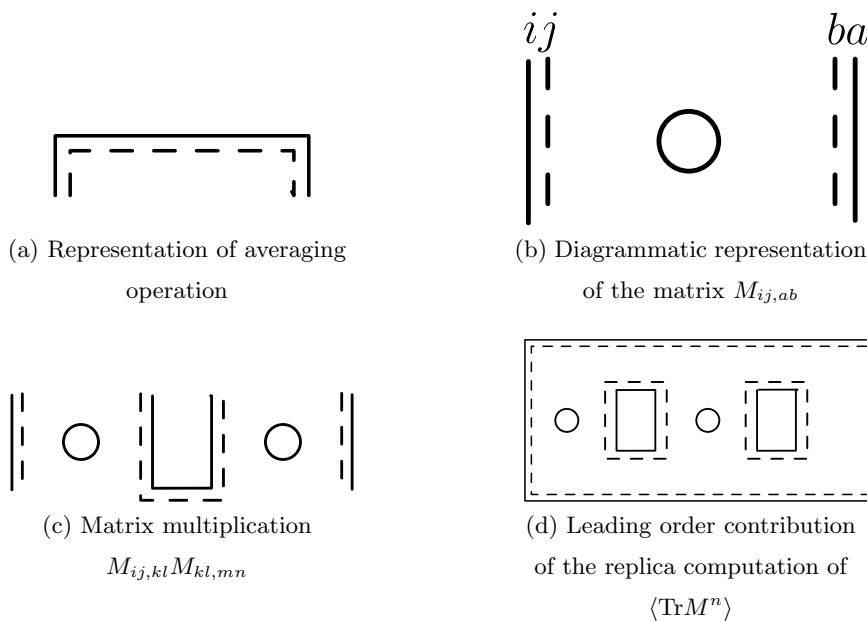


Figure 12: Diagrammatic representation of the computation of pseudo-negativity in the large system limit. The solid/dashed line represents the state in system A/B , respectively. The matrix M in Eq.(5.15) is represented by Figure 12b and the circle at the center denotes the thermal factors in M . The diagrammatic rule of contracting states is that each loop formed by the solid/dashed line gives a factor of d_A/d_B . The matrix product is represented in Figure 12c where the underline connects two states. The averaging operation is represented by a connected overhead line as in 12a. When the averaging line is connected across m number of matrices M s, the overall contribution coming from averaging over the thermal factors in the “half-loop” gives a factor of $Z(2m\beta)$. The quantity that we aim to compute is given in Figure 12d where only the first two matrices of the n matrices M of the diagrammatic representation is drawn. This particular choice of averaging (the way that the overhead line is connected) provides the leading contribution in the large d limit.

- [11] S. Ryu and T. Takayanagi, *Holographic derivation of entanglement entropy from AdS/CFT*, *Phys. Rev. Lett.* **96** (2006) 181602, [[hep-th/0603001](#)].
- [12] S. Ryu and T. Takayanagi, *Aspects of Holographic Entanglement Entropy*, *JHEP* **08** (2006) 045, [[hep-th/0605073](#)].
- [13] H. Liu and S. J. Suh, *Entanglement growth during thermalization in holographic systems*, *Phys. Rev. D* **89** (2014), no. 6 066012, [[arXiv:1311.1200](#)].
- [14] H. Liu and S. J. Suh, *Entanglement Tsunami: Universal Scaling in Holographic Thermalization*, *Phys. Rev. Lett.* **112** (2014) 011601, [[arXiv:1305.7244](#)].

- [15] R. Fan, P. Zhang, H. Shen, and H. Zhai, *Out-of-Time-Order Correlation for Many-Body Localization*, *Sci. Bull.* **62** (2017) 707–711, [[arXiv:1608.01914](#)].
- [16] M. Mezei and D. Stanford, *On entanglement spreading in chaotic systems*, *JHEP* **05** (2017) 065, [[arXiv:1608.05101](#)].
- [17] Z. D. Shi, S. Vardhan, and H. Liu, *Local dynamics and the structure of chaotic eigenstates*, [arXiv:2306.08032](#).
- [18] D. E. Parker, X. Cao, A. Avdoshkin, T. Scaffidi, and E. Altman, *A Universal Operator Growth Hypothesis*, *Phys. Rev. X* **9** (2019), no. 4 041017, [[arXiv:1812.08657](#)].
- [19] S.-K. Jian, B. Swingle, and Z.-Y. Xian, *Complexity growth of operators in the SYK model and in JT gravity*, *JHEP* **03** (2021) 014, [[arXiv:2008.12274](#)].
- [20] E. Rabinovici, A. Sánchez-Garrido, R. Shir, and J. Sonner, *Operator complexity: a journey to the edge of Krylov space*, *JHEP* **06** (2021) 062, [[arXiv:2009.01862](#)].
- [21] A. Dymarsky and M. Smolkin, *Krylov complexity in conformal field theory*, *Phys. Rev. D* **104** (2021), no. 8 L081702, [[arXiv:2104.09514](#)].
- [22] C. Liu, H. Tang, and H. Zhai, *Krylov complexity in open quantum systems*, *Phys. Rev. Res.* **5** (2023), no. 3 033085, [[arXiv:2207.13603](#)].
- [23] K. Adhikari, S. Choudhury, and A. Roy, *Krylov Complexity in Quantum Field Theory*, *Nucl. Phys. B* **993** (2023) 116263, [[arXiv:2204.02250](#)].
- [24] E. Rabinovici, A. Sánchez-Garrido, R. Shir, and J. Sonner, *Krylov complexity from integrability to chaos*, *JHEP* **07** (2022) 151, [[arXiv:2207.07701](#)].
- [25] A. Bhattacharyya, D. Ghosh, and P. Nandi, *Operator growth and Krylov complexity in Bose-Hubbard model*, *JHEP* **12** (2023) 112, [[arXiv:2306.05542](#)].
- [26] A. Bhattacharyya, S. S. Haque, G. Jafari, J. Murugan, and D. Rapotu, *Krylov complexity and spectral form factor for noisy random matrix models*, *JHEP* **10** (2023) 157, [[arXiv:2307.15495](#)].
- [27] T. Li and L.-H. Liu, *Inflationary Krylov complexity*, [arXiv:2401.09307](#).
- [28] A. M. García-García and J. J. M. Verbaarschot, *Spectral and thermodynamic properties of the Sachdev-Ye-Kitaev model*, *Phys. Rev. D* **94** (2016), no. 12 126010, [[arXiv:1610.03816](#)].
- [29] J. S. Cotler, G. Gur-Ari, M. Hanada, J. Polchinski, P. Saad, S. H. Shenker, D. Stanford, A. Streicher, and M. Tezuka, *Black Holes and Random Matrices*, *JHEP* **05** (2017) 118, [[arXiv:1611.04650](#)]. [Erratum: *JHEP* 09, 002 (2018)].
- [30] T. Li, J. Liu, Y. Xin, and Y. Zhou, *Supersymmetric SYK model and random matrix theory*, *JHEP* **06** (2017) 111, [[arXiv:1702.01738](#)].

- [31] J. Liu, *Spectral form factors and late time quantum chaos*, *Phys. Rev. D* **98** (2018), no. 8 086026, [[arXiv:1806.05316](#)].
- [32] R. de Mello Koch, J.-H. Huang, C.-T. Ma, and H. J. R. Van Zyl, *Spectral Form Factor as an OTOC Averaged over the Heisenberg Group*, *Phys. Lett. B* **795** (2019) 183–187, [[arXiv:1905.10981](#)].
- [33] C.-T. Ma and C.-H. Wu, *Quantum Entanglement and Spectral Form Factor*, *Int. J. Theor. Phys.* **61** (2022), no. 12 272, [[arXiv:2007.00855](#)].
- [34] A. Bhattacharyya, S. Ghosh, and S. Pal, *Aspects of $T\bar{T} + J\bar{T}$ deformed 2D topological gravity : from partition function to late-time SFF*, [arXiv:2309.16658](#).
- [35] Y. Nakata, T. Takayanagi, Y. Taki, K. Tamaoka, and Z. Wei, *New holographic generalization of entanglement entropy*, *Phys. Rev. D* **103** (2021), no. 2 026005, [[arXiv:2005.13801](#)].
- [36] A. Mollabashi, N. Shiba, T. Takayanagi, K. Tamaoka, and Z. Wei, *Pseudo Entropy in Free Quantum Field Theories*, *Phys. Rev. Lett.* **126** (2021), no. 8 081601, [[arXiv:2011.09648](#)].
- [37] A. Mollabashi, N. Shiba, T. Takayanagi, K. Tamaoka, and Z. Wei, *Aspects of pseudoentropy in field theories*, *Phys. Rev. Res.* **3** (2021), no. 3 033254, [[arXiv:2106.03118](#)].
- [38] K. Doi, J. Harper, A. Mollabashi, T. Takayanagi, and Y. Taki, *Pseudoentropy in dS/CFT and Timelike Entanglement Entropy*, *Phys. Rev. Lett.* **130** (2023), no. 3 031601, [[arXiv:2210.09457](#)].
- [39] Z. Li, Z.-Q. Xiao, and R.-Q. Yang, *On holographic time-like entanglement entropy*, *JHEP* **04** (2023) 004, [[arXiv:2211.14883](#)].
- [40] K. Doi, J. Harper, A. Mollabashi, T. Takayanagi, and Y. Taki, *Timelike entanglement entropy*, *JHEP* **05** (2023) 052, [[arXiv:2302.11695](#)].
- [41] X. Jiang, P. Wang, H. Wu, and H. Yang, *Timelike entanglement entropy in dS_3/CFT_2* , *JHEP* **08** (2023) 216, [[arXiv:2304.10376](#)].
- [42] X. Jiang, P. Wang, H. Wu, and H. Yang, *Timelike entanglement entropy and TT^- deformation*, *Phys. Rev. D* **108** (2023), no. 4 046004, [[arXiv:2302.13872](#)].
- [43] D. Chen, X. Jiang, and H. Yang, *Holographic TT^- deformed entanglement entropy in dS_3/CFT_2* , *Phys. Rev. D* **109** (2024), no. 2 026011, [[arXiv:2307.04673](#)].
- [44] I. Akal, T. Kawamoto, S.-M. Ruan, T. Takayanagi, and Z. Wei, *Page curve under final state projection*, *Phys. Rev. D* **105** (2022), no. 12 126026, [[arXiv:2112.08433](#)].
- [45] W.-z. Guo, S. He, and Y.-X. Zhang, *On the real-time evolution of pseudo-entropy in 2d CFTs*, *JHEP* **09** (2022) 094, [[arXiv:2206.11818](#)].
- [46] W.-z. Guo, S. He, and Y.-X. Zhang, *Constructible reality condition of pseudo entropy via pseudo-Hermiticity*, *JHEP* **05** (2023) 021, [[arXiv:2209.07308](#)].

- [47] S. He, J. Yang, Y.-X. Zhang, and Z.-X. Zhao, *Pseudo-entropy for descendant operators in two-dimensional conformal field theories*, [arXiv:2301.04891](#).
- [48] S. He, J. Yang, Y.-X. Zhang, and Z.-X. Zhao, *Pseudo entropy of primary operators in $T\bar{T}/J\bar{T}$ -deformed CFTs*, [arXiv:2305.10984](#).
- [49] K. Goto, M. Nozaki, and K. Tamaoka, *Subregion spectrum form factor via pseudoentropy*, *Phys. Rev. D* **104** (2021), no. 12 L121902, [[arXiv:2109.00372](#)].
- [50] S. Xu, L. Susskind, Y. Su, and B. Swingle, *A Sparse Model of Quantum Holography*, [arXiv:2008.02303](#).
- [51] A. M. García-García, Y. Jia, D. Rosa, and J. J. M. Verbaarschot, *Sparse Sachdev-Ye-Kitaev model, quantum chaos and gravity duals*, *Phys. Rev. D* **103** (2021), no. 10 106002, [[arXiv:2007.13837](#)].
- [52] E. Cáceres, A. Misobuchi, and A. Raz, *Spectral form factor in sparse SYK models*, *JHEP* **08** (2022) 236, [[arXiv:2204.07194](#)].
- [53] E. Cáceres, T. Guglielmo, B. Kent, and A. Misobuchi, *Out-of-time-order correlators and Lyapunov exponents in sparse SYK*, [arXiv:2306.07345](#).
- [54] E. Cáceres, A. Misobuchi, and R. Pimentel, *Sparse SYK and traversable wormholes*, *JHEP* **11** (2021) 015, [[arXiv:2108.08808](#)].
- [55] D. Jafferis, A. Zlokapa, J. D. Lykken, D. K. Kolchmeyer, S. I. Davis, N. Lauk, H. Neven, and M. Spiropulu, *Traversable wormhole dynamics on a quantum processor*, *Nature* **612** (2022), no. 7938 51–55.
- [56] M. Tezuka, O. Oktay, E. Rinaldi, M. Hanada, and F. Nori, *Binary-coupling sparse Sachdev-Ye-Kitaev model: An improved model of quantum chaos and holography*, *Phys. Rev. B* **107** (2023), no. 8 L081103, [[arXiv:2208.12098](#)].
- [57] A. Kitaev, *Hidden correlations in the Hawking radiation and thermal noise*, *Talk at KITP*.
- [58] A. Kitaev, *A simple model of quantum holography*, *Talk at KITP*.
- [59] J. Maldacena and D. Stanford, *Remarks on the Sachdev-Ye-Kitaev model*, *Phys. Rev. D* **94** (2016), no. 10 106002, [[arXiv:1604.07818](#)].
- [60] T. Kanazawa and T. Wettig, *Complete random matrix classification of SYK models with $\mathcal{N} = 0, 1$ and 2 supersymmetry*, *JHEP* **09** (2017) 050, [[arXiv:1706.03044](#)].
- [61] F. Sun and J. Ye, *Periodic Table of the Ordinary and Supersymmetric Sachdev-Ye-Kitaev Models*, *Phys. Rev. Lett.* **124** (2020), no. 24 244101, [[arXiv:1905.07694](#)].
- [62] Y. Y. Atas, E. Bogomolny, O. Giraud, and G. Roux, *Distribution of the ratio of consecutive level spacings in random matrix ensembles*, *Phys. Rev. Lett.* **110** (Feb, 2013) 084101.

- [63] M. Hanada, A. Jevicki, X. Liu, E. Rinaldi, and M. Tezuka, *A model of randomly-coupled Pauli spins*, [arXiv:2309.15349](#).
- [64] J. Cotler, N. Hunter-Jones, J. Liu, and B. Yoshida, *Chaos, Complexity, and Random Matrices*, *JHEP* **11** (2017) 048, [[arXiv:1706.05400](#)].
- [65] Y. Alhassid, *The Statistical theory of quantum dots*, *Rev. Mod. Phys.* **72** (2000) 895–968, [[cond-mat/0102268](#)].
- [66] L. D’Alessio, Y. Kafri, A. Polkovnikov, and M. Rigol, *From quantum chaos and eigenstate thermalization to statistical mechanics and thermodynamics*, *Adv. Phys.* **65** (2016), no. 3 239–362, [[arXiv:1509.06411](#)].
- [67] H. Shapourian, S. Liu, J. Kudler-Flam, and A. Vishwanath, *Entanglement Negativity Spectrum of Random Mixed States: A Diagrammatic Approach*, *PRX Quantum* **2** (2021), no. 3 030347, [[arXiv:2011.01277](#)].
- [68] N. Dowling, P. Kos, and K. Modi, *Scrambling is Necessary but Not Sufficient for Chaos*, [arXiv:2304.07319](#).
- [69] D. A. Roberts, D. Stanford, and A. Streicher, *Operator growth in the SYK model*, *JHEP* **06** (2018) 122, [[arXiv:1802.02633](#)].
- [70] D. A. Roberts and D. Stanford, *Two-dimensional conformal field theory and the butterfly effect*, *Phys. Rev. Lett.* **115** (2015), no. 13 131603, [[arXiv:1412.5123](#)].
- [71] C. H. Bennett, G. Brassard, S. Popescu, B. Schumacher, J. A. Smolin, and W. K. Wootters, *Purification of noisy entanglement and faithful teleportation via noisy channels*, *Phys. Rev. Lett.* **76** (1996) 722–725, [[quant-ph/9511027](#)].
- [72] A. Peres, *Separability criterion for density matrices*, *Phys. Rev. Lett.* **77** (1996) 1413–1415, [[quant-ph/9604005](#)].
- [73] P. Calabrese, J. Cardy, and E. Tonni, *Entanglement negativity in quantum field theory*, *Phys. Rev. Lett.* **109** (2012) 130502, [[arXiv:1206.3092](#)].
- [74] Y. Kusuki, J. Kudler-Flam, and S. Ryu, *Derivation of holographic negativity in AdS_3/CFT_2* , *Phys. Rev. Lett.* **123** (2019), no. 13 131603, [[arXiv:1907.07824](#)].
- [75] A. R. Brown, D. A. Roberts, L. Susskind, B. Swingle, and Y. Zhao, *Holographic Complexity Equals Bulk Action?*, *Phys. Rev. Lett.* **116** (2016), no. 19 191301, [[arXiv:1509.07876](#)].
- [76] A. R. Brown, D. A. Roberts, L. Susskind, B. Swingle, and Y. Zhao, *Complexity, action, and black holes*, *Phys. Rev. D* **93** (2016), no. 8 086006, [[arXiv:1512.04993](#)].
- [77] A. Belin, R. C. Myers, S.-M. Ruan, G. Sárosi, and A. J. Speranza, *Does Complexity Equal Anything?*, *Phys. Rev. Lett.* **128** (2022), no. 8 081602, [[arXiv:2111.02429](#)].